Surface-to-volume ratio: How building geometry impacts solar energy production and heat gain through envelopes

IOP Conf. Series: Earth and Environmental Science **323** (2019) 012034 doi:10.1088/1755-1315/323/1/012034

Surface-to-volume ratio: How building geometry impacts solar energy production and heat gain through envelopes

Araji M T

Environmental Design Program, Faculty of Architecture, University of Manitoba, 201 John A. Russell Building, Winnipeg, MB R3T 2N2 Canada

Mohamad.Araji@umanitoba.ca

Abstract. This paper explored the relationship between building geometry and renewable energy production of building-integrated photovoltaics (BIPV). Heat gain was incorporated as a conflicting constraint with respect to energy performance. The building façade was mathematically analyzed by taking into account heat transfer pertaining to site conditions along with different parameters that included shading, orientation, PV tilts (β) and surface-to-volume ratio (S/V) as a measure of building compactness. The study involved calculating the impact of each parameter on the convection, conduction and radiation components of the incoming solar energy. S/V was shown to be directly proportional to the amount of solar energy received by the façades and gained by the building in the form of heat. The positive correlation of heat gain with S/V was nearly linear with a slope of around 41.8 kWh/m^2/m^{-1} and a mean of approximately 3.4 times more. With the most suitable geometry in terms of net energy gain, S/V of 0.14 m^{-1} yielded the highest difference between energy production and heat gain. In terms of β, the results demonstrated negative slope of energy production with respect to the tilt at about 2.12 times higher than that displayed by heat gain. Accounting for inter-building effects, a shading reduction equal to d percent can be estimated to an increase of $1.37d$ degrees in β at a building consumption of 60 kWh/m^2.

List of Abbreviations

H	Shading factor
h	Building height
E	Illuminance
C	Building consumption
E_e	Irradiance
v	Human sensitivity
λ	wavelength
Λ	Range of wavelengths from 450 nm to 750 nm
w	Length of the East-West façade
l	Length of the North-South façade
S/V	Surface-area-to-volume ratio
β	PV tilt
F_s	View factor from sky to PV surface
F_g	View factor from PV surface to ground
A_{facade}	Total area of façade
E_{prod}	Production from building integrated renewable energy
Q_{facade}	Heat gain through the façade per unit area
Q_{solar}	Heat gain through solar irradiation
Q_{cond}	Heat gain through conduction
U	The surface U-value
T_{out}	Outside temperature
T_{in}	Inside temperature
$Q_{solar,b}$	Heat gain through E_B
$Q_{solar,d}$	Heat gain through E_{diff}
$Q_{solar,r}$	Heat gain through E_r
$SHGC_\beta$	Solar Heat Gain Coefficient, dependent on β
E_B	Beam component of solar irradiation
E_{diff}	Diffused component of solar irradiation
E_r	Reflected component of solar irradiation

1. Introduction

BIPV's influence on the heat transfer through the building's envelope has been significant. This is because solar cell surfaces affect the overall thermal resistance of the envelope. Comparisons of energy performance and building cooling and heating loads were performed in [1]. Non-ventilated air duct BIPV was shown to have highest power output and lowest heat transfer. Hot wire anemometry measurements, coupled with CFD computations were utilized to calculate heat transfer coefficients in a BIPV/T setting [2]. It was concluded that heat transfer characteristics of PV's internal surface play a critical role in the performance of the façade. The impact of climate on BIPV production was studied in [3]. It was concluded that output is maximized on cold, clear days. Also, snow was found to be a positive factor in production since it can reflect light on to the solar panel from other surfaces. Using a series of experiments, a non-linear stochastic differential equation was developed for the heat transfer of a BIPV component [4]. The method was shown to be useful in modelling nonlinear stochastic thermal phenomena in BIPV systems. The impact of surface temperature of BIPV was mathematically investigated in [5]. It was established that heat transfer increased with forced ventilation, and a high forced velocity in the

air gap contributed to increased heat transfer from the BIPV unit. A simulation model aimed at predicting energy production, thermal behaviour and transient interaction with the building envelope was presented in [6]. The accuracy of the model regarding surface temperatures was close to 0.6^oC, while for air temperature at the outlet of the system, the accuracy was slightly less than 1^oC. Suitability of BIPV in terms of thermal performance was studied in [7]. The study was based on real-time data monitoring supported by computer-based building simulation model. It was concluded that PV as a roofing material caused significant thermal discomfort to the occupants. A fully coupled PV model, integrated in a building simulation code was used to predict the temperature field in the complex wall constituted by BIPV façade in [8]. It was concluded that the performance of the BIPV was greatly dependant on the radiative heat transfer within the semi-transparent layers and the convective heat transfer in the fluid layers.

In terms of building form utilizations, the associated optimum geometry and composition in the presence of BIPV is still limited. Bostancioglu [9] confirmed that the building form along with thermophysical features of the envelope are among the significant factors affecting a building's energy performance. Depecker et al. [10] studied the ratio of the external skin surface and inner volume of the building as a representation of building geometry. This ratio was found to be inversely proportional to building's energy consumption in cold and scarcely sunny winters. A one-dimensional transient model for a BIPV system resulted in an overall energy efficiency of 53.7% by applying the PV modules for a fixed building form [11]. Hemsath et al. [12] studied energy consumption with multiple building geometry variations and material considerations. The outcomes of their research stressed the significance of formal variations in the early design phase to inform decision-making for best building performance. Hwang et al. [13] showed an analytic optimization for PV modules inclinations with relevant spacing between them in building façades. A genetic algorithm was recently developed to help designers determine the optimal envelope geometries with BIPV while considering the net building energy performance with both consumption and generation as the evaluation criteria [14]. The study tested features such as building dimensions, window-to-wall-ratio, orientation, and PV alignment.

Overall, focusing on the specification of PV components in relation to the envelope is no longer sufficient. There is a need for computational methods to advance building form optimization while integrating renewables for zero energy targets. Energy generation and heat gain have been studied separately in terms of the building geometry. This paper aims to answer the novel question of how to seek the most optimal geometry that *jointly* optimizes the conflicting constraints of BIPV performance and heat gain through the façade. Since there is no closed-form relationship between a building's geometry and these constraints, numerical studies are presented to estimate this correlation. The analysis involves mathematical modeling of parameters specific to additional contextual boundary factors of building consumption with various programs and forms with their applicability and feasibility analysis.

2. Methodology

A mathematical model is extended in the following subsections to examine the energy performance as related to building design optimization and integrated PV. The work comprises of procedures for heat gain calculation and the influence of building geometry.

2.1. Heat Gain Calculation

Let the rate of heat gain through the façade per unit area be given by $\dot{Q}_{facade}$ (units: W/m^2). Then,

$$\dot{Q}_{facade} = \dot{Q}_{solar} + \dot{Q}_{cond}, \tag{1}$$

where Q_{solar} and Q_{cond} represent the heat gain through solar irradiation and conduction respectively, and the dot operator is used to represent the rate. $\dot{Q}_{cond}$ depends on the U-value of the surface and the temperature difference across it:

$$\dot{Q}_{cond} = U(T_{out} - T_{in}), \tag{2}$$

where U, T_{out} and T_{in} represent the surface U-value (units: W/m^{2}K), outside temperature(units: K) and inside temperature(units: K) respectively.

The heat gain through solar irradiation is a product of incident solar irradiation and the solar heat gain coefficient (SHGC) of the surface. In order to account for $\dot{Q}_{solar}$, components of irradiation (beam, diffused and reflected) should be separately accounted for. In other words, $\dot{Q}_{solar}$ can be written as

$$\dot{Q}_{solar} = \dot{Q}_{solar,b} + \dot{Q}_{solar,d} + \dot{Q}_{solar,r}, \tag{3}$$

where $Q_{solar,b}$, $Q_{solar,d}$ and $Q_{solar,r}$ represent the heat gain through the beam, diffused and reflected components of solar irradiation (denoted by E_B, E_{diff} and E_r respectively). Studies have shown that SHGC for $Q_{solar,b}$ depends on the tilt of the surface [15]. $Q_{solar,b}$ will also be affected by the shading coefficient H. Thus,

$$\dot{Q}_{solar,b} = SHGC_\beta \cdot E_B \cdot H, \tag{4}$$

where the subscript β with SHGC is there to show the former's dependence on the latter. H takes values between 0 and 1, where 0 implies complete shading and 1 implies no shading. $\dot{Q}_{solar,d}$ is given by

$$\dot{Q}_{solar,d} = SHGC \cdot E_{diff} \cdot F_s, \tag{5}$$

where F_s is the sky view factor given by $F_s = \frac{1+\cos\beta}{2}$. $Q_{solar,r}$ is given by

$$\dot{Q}_{solar,r} = SHGC \cdot E_r \cdot F_g = SHGC \cdot \rho_g E_B \cdot F_g, \tag{6}$$

where ρ_g is the reflection coefficient (typically set as 0.2), and F_g is the view factor from the ground given by $F_g = \frac{1-\cos\beta}{2}$. Plugging Eqs. (2), (3), (4), (5) and (6) in Eq. (1), the total heat gain per unit area through the façade can be summarized as:

$$\dot{Q}_{facade} = SHGC_\beta \cdot E_B \cdot H + SHGC \cdot E_{diff} \cdot F_s + SHGC \cdot \rho_g E_B \cdot F_g + U(T_{out} - T_{in}). \tag{7}$$

The convention to calculate $SHGC_\beta$ utilizes angle correction factors [16]. If the correction factor for a specific β is given by f_β, then $SHGC_\beta = f_\beta \cdot SHGC$.

In conjunction with the above analysis on irradiation, a similar analysis can be done on lighting by noting that illuminance is obtained by averaging irradiance over the sensitivity of human eye for the full spectrum of wavelengths [17]. In other words,

$$E = 683 \cdot H \int_{\lambda \in \Lambda} E_e(\lambda) v(\lambda) d\lambda. \tag{8}$$

where E represents illuminance (units: lux), $E_e(\lambda)$ represents spectral irradiance (units: W/m^2), v represents human sensitivity, λ represents wavelength (units: m) and Λ represents the range of wavelengths from 450 nm to 700 nm, where spectral efficiency is prominent [17]. It is clear from Eq. (4) and Eq. (8) that the effect of shading on lighting will be similar to that on irradiance, i.e., shading factor H acts as a proportionality constant in both cases. This is in alignment with studies reported in the literature [18].

2.2. Influence of Building Geometry

It is noteworthy that $\dot{Q}_{facade}$ in Eq. (7) is represented per unit area. However, area of the façade alone does not provide the complete picture of a building performance in terms of its heat gain and energy production. Let E_{prod} (units: kWh/m^2) denote the energy production per unit area from the PV panels installed on the building's façade. Figure 1 shows two cases to demonstrate the influence of building's geometry. In the first case, two buildings with equal occupancy but unequal façade area (A_{facade}) are shown. In the second case, the reverse case is shown (unequal occupancy and equal A_{facade}). Both these cases allude to some correlation between a building's performance per capita and its compactness. A suitable measure of building's compactness is the surface-area-to-volume-ratio (S/V) which is defined as the ratio of A_{facade} to the volume of the building. For a rectangular building, this can be given by,

$$S/V = \frac{A_{facade}}{lwh} = \frac{2lh+2wh}{lwh} = \frac{2}{w} + \frac{2}{l}. \tag{9}$$

A similar relationship between building shape and heat transfer through its façade is reported in [19], where the author used the term shape coefficient to represent the ratio of façade and roof surface area to its volume. In Figure 1, both cases yield a higher energy production and heat gain per capita when S/V is higher.

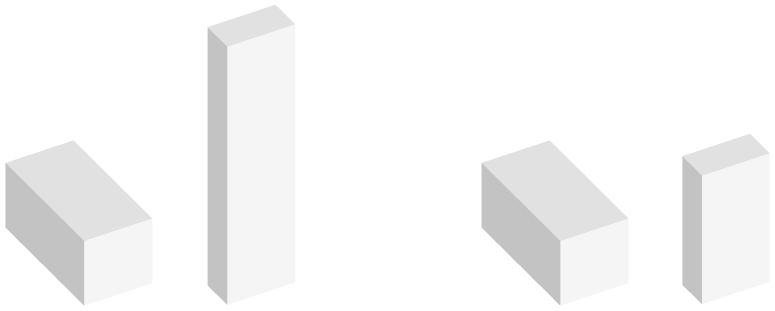

	Case 1		Case 2	
Width x Length x Height	1 x 2 x 1	1 x ½ x 4	1 x 2 x 1	1 x ½ x 2
Volume (cubic unit)	2	2	2	1
Façade Area (square unit)	8	12	6	6

Figure 1: Case 1: Equal volume but different façade areas. Case 2: Equal façade areas but different volume.

2.3. Assumptions and Input Parameters

To apply the mathematical model, some parameters need to be specified. For application purposes, the city of Chicago in the United States of America was considered with a latitude

41.87^{o}N and longitude 87.62^{o}W and a six-hour lag from Greenwich. The average solar irradiation on the PV modules was 2 to 3 kWh/m^2/day and the climate was classified as continental. Building orientation and PV tilt ranged from 0^o to 90^o and from site's latitude to vertical façade's application, respectively. T_{out} is taken to be 27^{o}C, which is the average temperature in Chicago for the month of August. T_{in} was chosen as 23^{o}C; typical indoor temperature. The U-value for a typical double glazed unit plus a transparent PV module was selected to be 1.2 kW/m^2 [20].

3. Result and Discussion

The positive correlation between a building's performance and its S/V value cannot be expressed in closed form analytically. However, numerical evaluation is conveniently done by changing l, w and h is equal proportions for E_{prod}, Q_{facade} and S/V. This trend is shown in Figure 2a, where the optimum number of occupants per square meter have been chosen to be 0.0286 [21]. The trend of Q_{facade} is fairly linear with a slope of 41.8. However, the behavior of E_{prod} can be divided into two separate (almost linear) regions. For $S/V < 0.13$, the slope of E_{prod} is steep with a value of 405, while for $S/V > 0.13$, slope decreases to about 30. Given that Q_{facade} contributes to the overall building consumption C, an optimum building geometry should be sought that maximizes the difference between E_{prod} and Q_{facade}. This difference is shown in Figure 2b. It can be observed that the relationship between S/V and $E_{prod} - Q_{facade}$ follows a convex path with a global maximum at some intermediate value (0.1407 in this case). It follows that the most optimal geometry for a building in terms of its energy performance and heat transfer will have S/V that maximizes $E_{prod} - Q_{facade}$. In order to achieve S/V values shown in Figure 2b, a range of values of h, l and w are $h \in [20, 200]$(units: m), $lw = Area \in [400, 2000]$ (units: m^2) and $AR = \frac{l}{w} \in [1, 10]$ (unitless).

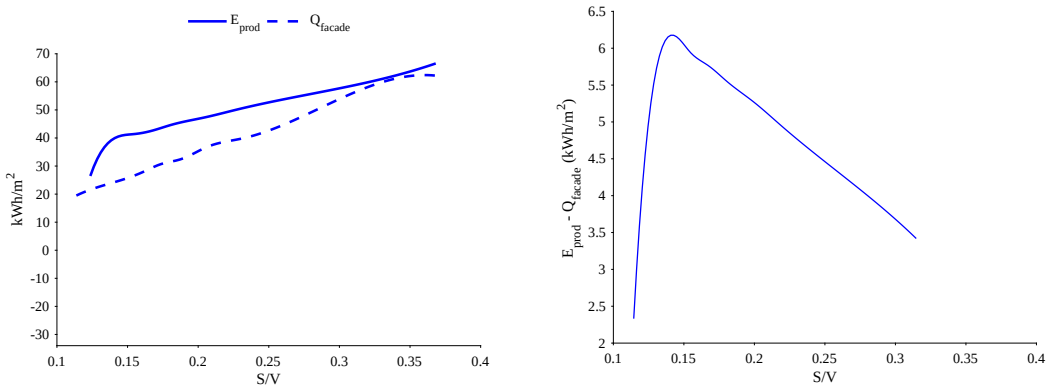

Figure 2: (a: Left) E_{prod} and Q_{facade} vs S/V (b: Right) S/V vs $E_{prod} - Q_{facade}$.

It is noteworthy from Eq. (9) that a specific value of S/V can be achieved by an infinite combinations of h, l and w. This flexibility is useful in case of any practical constraints that may limit a building's area or height. $E_{prod} - Q_{facade}$ starts from a minimum and increases linearly with a slope of about 8.45 before reaching its maximum of 98,700 kWh/person. Then, $E_{prod} - Q_{facade}$ begins to decrease in a non-linear fashion before reaching the minimum value at S/V of 0.28.

The dependence of β on Q_{facade} is evident from Eq. (7). Additionally, E_{prod} also depends on β since the incident angle of solar irradiation directly influences the amount of energy generated.

The quantification of this dependence is shown in Figure 3 for a south facing façade surface at a site location of latitude 41^o. E_b is calculated to be 23.93 kWh/m^2 through ASHRAE [22], and E_{diff} is taken to be 45% of E_b [23]. It is clear that $\beta = 40^o$ yields the highest energy production. This is in confirmation with the literature, that reports the site's latitude to be the most productive value of β [24]. The decrease in E_{prod} with β is observed to be almost linear. For every d unit increase in β, E_{prod} decreases by $28.3d$ units. With respect to Q_{facade}, the trend is constant till $\beta = 65^o$, after which it starts decreasing with a slope of 13.47 units.

In order to study the inter-building effects on BIPV production, Figure 4 displays the range of achievable energy thresholds as a function of β and H. These thresholds refer to the percentage of energy produced compared to the total consumption of 40 kWh/m^2 and 60 kWh/m^2. A threshold level of 100% or more would correspond to meeting the net-zero criterion. For each β, the lower and upper boundaries of the region correspond to full shading ($H = 0$) and no shading ($H = 1$) respectively. As β moves away from the site's latitude, shading level should decrease to stay at the same threshold level. For example, at 60% level and $C = 60$ kWh/m^2, $\beta = 40.6^o$ can allow for 59% shading, while $\beta = 89.9^o$ allows for only 15% shading. The net-zero region can be achieved for ($\beta < 49.49^o$, $H > 0.91$) for $C = 60$ kWh/m^2 and ($\beta < 90^o$, $H > 0.48$) for $C = 40$ kWh/m^2 as shown in the shaded region.

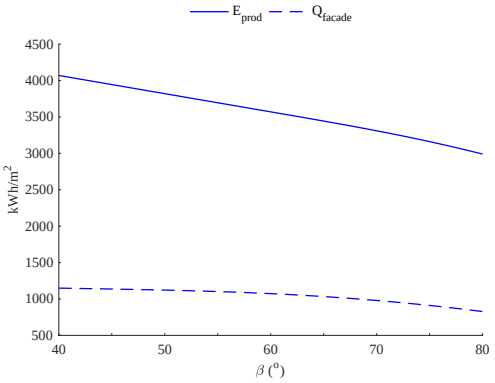

Figure 3: E_{prod} and Q_{facade} for various values of β.

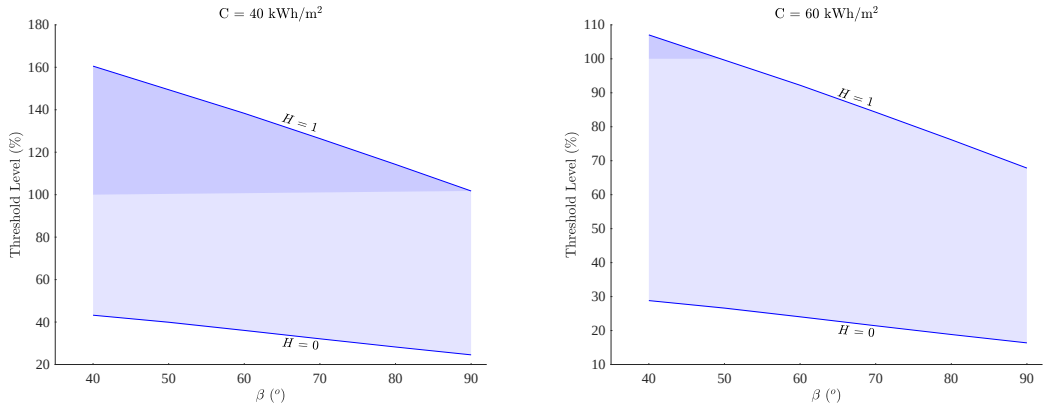

Figure 4: Energy production thresholds with shading factor H and tilt angle β. The darker region corresponds to fulfilling the net-zero criterion.

4. Conclusion

The design and implementation procedure of BIPV as a renewable energy system was carried out in order to find its best performance with various building conditions, taking into consideration comparison between different façade applications, orientations, and relevant tilt angles. In terms of parameters, the most effective methods of maximizing PV's energy production would involve factors such as specification of the building's surface-to-volume ratio (S/V), orientation, and the effect of PV tilt angle (β) on energy targets. The goal of this work was to establish a mathematical relationship for the heat transfer through a BIPV façade system. To this end, components of conduction and radiation were separately considered, and the dependence of β on the radiation component through the solar heat gain coefficient was described in detail.

This paper linked the BIPV performance to heat gain through the building envelope. It is suggested that heat gain is directly proportional. There is a considerable utility with such multidimensional problem of maximizing energy production and minimizing heat gain. Both E_{prod} and Q_{facade} were shown to be directly proportional to S/V. The positive correlation of Q_{facade} with S/V was nearly linear with a slope of around 41.8 kWh/m^2/m^{-1}. The average positive correlation of E_{prod} with S/V was approximately 3.4 times higher. The difference of E_{prod} and Q_{facade} was analyzed against S/V to investigate the most suitable geometry in terms of net energy gain. It was found that under continental conditions considered, S/V of 0.14 m^{-1} yielded the highest difference between energy production and heat gain. In terms of PV tilt β, the results demonstrated that both E_{prod} and Q_{facade} are maximized when β is close to the site's latitude. The negative slope of E_{prod} with respect to β was about 2.12 times higher than that displayed by Q_{facade}, concluding that the site's latitude is most optimal in terms of $E_{prod} - Q_{facade}$.

5. References

[1] Yiping Wang, Wei Tian, Jianbo Ren, Li Zhu, and Qingzhao Wang. Influence of a building's integrated-photovoltaics on heating and cooling loads. *Applied energy*, 83(9):989–1003, 2006.

[2] Rafaela A Agathokleous and Soteris A Kalogirou. Double skin facades (dsf) and building integrated photovoltaics (BIPV): A review of configurations and heat transfer characteristics. *Renewable Energy*, 89:743–756, 2016.

[3] Steven Strong. Building integrated photovoltaics (BIPV). *Whole building design guide*, 9, 2010.

[4] Emrah Biyik, Mustafa Araz, Arif Hepbasli, Mehdi Shahrestani, Runming Yao, Li Shao, Emmanuel Essah, Armando C Oliveira, Teodosio del Caño, Elena Rico, et al. A key review of building integrated photovoltaic (BIPV) systems. *Engineering Science and Technology, an International Journal*, 20(3):833–858, 2017.

[5] Nynne Friling, María José Jiménez, Hans Bloem, and Henrik Madsen. Modelling the heat dynamics of building integrated and ventilated photovoltaic modules. *Energy and Buildings*, 41(10):1051–1057, 2009.

[6] Konstantinos ORDOUMPOZANI, Theodoros Theodosiou, Dimitrios Bouris, and Katerina Tsikaloudaki. Energy and thermal modeling of building façade integrated photovoltaics. *Thermal Science*, 22, 2018.

[7] Gayathri Aaditya and Monto Mani. BIPV: a real-time building performance study for a roof-integrated facility. *International journal of sustainable energy*, 37(3):249–267, 2018.

[8] Dimitri Bigot, Miranville Frédéric, Harry Boyer, and Ali Hamada Fakra. Thermal performance of photovoltaic systems integrated in buildings. In *Solar Collectors and Panels, Theory and Applications*. IntechOpen, 2010.

[9] E Bostancioğlu. Effect of building shape on a residential building's construction, energy and life cycle costs. *Architectural Science Review*, 53(4):441–467, 2010.

[10] Patrick Depecker, Christophe Menezo, Joseph Virgone, and Stephane Lepers. Design of buildings shape and energetic consumption. *Building and Environment*, 36(5):627–635, 2001.

[11] Basant Agrawal and GN Tiwari. Optimizing the energy and exergy of building integrated photovoltaic thermal (BIPVT) systems under cold climatic conditions. *Applied Energy*, 87(2):417–426, 2010.

[12] Timothy L Hemsath and Kaveh Alagheband Bandhosseini. Sensitivity analysis evaluating basic building geometry's effect on energy use. *Renewable Energy*, 76:526–538, 2015.
[13] Taeyon Hwang, Seokyoun Kang, and Jeong Tai Kim. Optimization of the building integrated photovoltaic system in office buildings. focus on the orientation, inclined angle and installed area. *Energy and Buildings*, 46:92–104, 2012.
[14] Amr Mamdoh Ali Youssef, Zhiqiang John Zhai, and Rabee Mohamed Reffat. Genetic algorithm based optimization for photovoltaics integrated building envelope. *Energy And Buildings*, 127:627–636, 2016.
[15] Christian Kohler, Yash Shukla, and Rajan Rawal. Calculating the effect of external shading on the solar heat gain coefficient of windows. 2017.
[16] Stephen J Harrison, Siman J van Wonderen, Roger Henry, Kenneth Elovitz, and Stephen Carpenter. Evaluation of solar heat gain coefficient for solar-control glazings and shading devices/discussion. *ASHRAE Transactions*, 104:1051, 1998.
[17] North American Philips Co and Philips photonics. *Photomultiplier Tubes: Principles & Applications*. Philips photonics. Philips Photonics International Marketing, 1993.
[18] Alex Ryer and Visible Light. Light measurement handbook. 1997.
[19] Guohui Feng, Shuai Sha, and Xiaolong Xu. Analysis of the building envelope influence to building energy consumption in the cold regions. *Procedia Engineering*, 146:244–250, 2016.
[20] Anatoli Chatzipanagi, Francesco Frontini, and Alessandro Virtuani. BIPV-temp: A demonstrative Building Integrated Photovoltaic installation. *Applied energy*, 173:1–12, 2016.
[21] Sara J Wilkinson and Richard G Reed. Office building characteristics and the links with carbon emissions. *Structural survey*, 24(3):240–251, 2006.
[22] K Bakirci. Estimation of solar radiation by using ASHRAE clear-sky model in erzurum, turkey. *Energy Sources, Part A*, 31(3):208–216, 2009.
[23] CJT Spitters, HAJM Toussaint, and J Goudriaan. Separating the diffuse and direct component of global radiation and its implications for modeling canopy photosynthesis part i. components of incoming radiation. *Agricultural and Forest Meteorology*, 38(1-3):217–229, 1986.
[24] MS Ismail, M Moghavvemi, and TMI Mahlia. Research of BIPV optimal tilted angle use of latitude concept for south orientated plans. *Energy Conversion and Management*, 73:10–16, 2013.